Fibers and Polymers 2021, Vol.22, No.11, 3120-3134
DOI 10.1007/s12221-021-0370-x

ISSN 1229-9197 (print version)
ISSN 1875-0052 (electronic version)

Effect of Micro-fillers on the Performance of Thermoplastic Para Aramid Composites for Impact Applications

Muhammad Imran Khan[1], Muhammad Umair[1], Rizwan Hussain[2], and Yasir Nawab[1]*

[1]*Textile Composite Materials Research Group, National Center for Composite Materials, Faculty of Engineering and Technology, National Textile University, Faisalabad 37610, Pakistan*
[2]*Lab for Advanced Materials Processing (LAMP), National Center for Physics, Islamabad 44000, Pakistan*
(Received December 7, 2020; Revised December 29, 2020; Accepted February 1, 2021)

Abstract: Para-aramid fiber reinforced composite are the premier choice for protective applications due to their superior mechanical properties. Use of thermoplastic matrices in such composites is gaining the interest of researchers due to their better energy absorption. Polyvinyl butyral (PVB), a thermoplastic matrix, has very good mechanical and impact properties. Many studies have reported in the literature on the characterization of mechanical performance of thermoset composites for impact applications, however, there is a need to study para-aramid (PA) thermoplastic composite produced with PVB as well as further improvement of their properties using particulate reinforcements. In the present work, prepreg were developed by impregnating PA woven fabrics with a slurry of PVB, with and without silica micro particles (SMP) and glass microspheres (GMS) ranging from 1-4 %. Composites were fabricated using compression molding. 3-point bending (flexural), Pendulum (Charpy) impact and drop weight impact testing of the composites were performed. The results showed that by the addition of SMP and GMS the impact properties were increases and GMS gives better results as compared to SMP. One-way ANOVA (Tukey) statistical analysis supports the experimental findings.

Keywords: Thermoplastic composite, Para-aramid, PVB, Micro-fillers, Mechanical performance

Introduction

Composite materials are used frequently as protection against impact. Depending upon level of protection, different materials can be used in different ways. High performance fibers such as Para aramid and Ultra High Molecular Weight Polyethylene are used as reinforcement in such composites. Fabric patterns such as 2D woven, 3D woven and unidirectional (UD's) are used to place fibers in a specific structure to achieve optimum protection. Both thermoset and thermoplastic resins have been reported in the literature [1,7] as matrix materials, with associated benefits and disadvantages. Different fillers are added to matrix to improve its properties [1].

Bullet resistant fabric is made from high tenacity fibers such as aramids (Kevlar, Technora, Tawron) [2-6] and ultrahigh molecular weight polyethylene (Spectra, Dyneema) [7]. Also, carbon, silk, e-glass [8], nylon and Zylon used in the manufacturing of body armors. The efficiency of ballistic resistant fabric depends upon the nature of yarn used, weave type and cover factor. Commonly, plain weave with dense square construction is used [9]. It is known that fabrics with a cover factor range 0.6-0.95 are efficient for ballistic protection [10]. Due to remarkable properties, Kevlar reinforced composites are being extensively used in ballistic protective application like hard and soft body armors etc. [11]. Armors made from Kevlar fiber can stop a bullet at a much lighter weight than polyamide fiber also backing of Kevlar fiber are being used with ceramic plates to stop a rifle bullet [12].

Kumar *et al.* [13] have investigated the mechanical properties of 2D woven thermoplastic composites. Three types of reinforcement fabrics were produced. Two fabrics were homogeneous plain-woven Kevlar and basalt fabrics, and third fabric was made from hybrid yarns (Kevlar and basalt yarns). Then their composites were made by using a polypropylene matrix. Composites made of hybrid yarns showed better tensile and in-plane compression properties than others.

There are two types of matrices; thermoset and thermoplastics used in composites for impact applications. Most commonly used thermoset matrix is epoxy. Thermosetting matrices are naturally liquid at room temperature [14]. Their crosslinking starts by the addition of initiator and hardener in it and then room temperature and post curing is done. Once they are crosslinked (completely cured), they cannot be melted. And this polymerization cannot be reversed. They are brittle materials. Few examples of these polymers are green epoxies, polyester, phenolic resins and vinyl ester etc. [15].

Thermoplastic matrices are solid at room temperature. They have linear and branched structures with no crosslinks [16]. An important property of thermoplastic materials is their flexibility that makes them impact resistant [17]. Also, Phillips *et al.* [18] consolidation mechanism of thermoplastic composites as a function of temperature, time and pressure was studied. Image analysis through optical microscopy and fracture tests were done. A model developed for intimate contact formation and auto-adhesion between adjacent plies of composite has good agreement with results.

*Corresponding author: yasir.nawab@yahoo.com

Kulkarnia *et al.* [19] worked on design, performance, and material of combat helmet. They observed ballistic energy absorption mechanism, helmet curvature effect on its performance and parameters for its performance measurement. They elaborated properties of conventionally used materials (Kevlar fibers and thermoset matrix) and new materials (thermoplastic materials and Nano composites) of the future. They concluded that carbon fiber/UHMWPE based composites can give a high level of protection with reduced weight. And nanocomposites with polymer matrix give the highest protection, but at the expense of cost.

Brown *et al*. [20] did numerical simulations of impact damage in thermoplastic composite. Thermoplastic composite has good application in vehicle bumper and front-end structure to increase pedestrian protection. Glass/polypropylene commingled fabric composite was made. A series of in-plane tension and compression test were performed and modeled through MAT 162 software. This software is a versatile tool for prediction of impact damage in thermoplastic composites.

Khondker *et al.* [21] investigated the mechanical properties of aramid/nylon, aramid epoxy knitted composites and their relationship to bonding between fiber and matrix. They concluded that aramid/nylon composites have a strong interracial interface between fiber and matrix than aramid/ epoxy composite for long molding time. Also, tensile strength decreases and tensile modulus increases with longer molding time.

Richter *et al.* [22] proposed that combining the two technologies lead to an efficient way of manufacturing a structural component part which consists of continuous thermoplastic (polyamide 6,6) and glass fiber. Continuous glass fiber reinforced polyamide 6.6 hybrid yarns and composites have high impact resistance, high stiffness, and strength values as well as short production cycle capabilities and low material costs.

Use of different fillers such as SiO_2 [23], TiO_2, ZnO, ZrO_2 [24], CuO, CNT's [8], Graphene, aluminum, gamma alumina, silicon carbide, colloidal silica and potato flour [25] and SiC [26,27] with different sizes and percentages along with thermoset matrices is already published in literature. For the improvement of mechanical and impact properties SiO2 is the most important and commonly used particles as secondary reinforcement.

It was reported that addition of silica particles, improves impact properties of Kevlar/epoxy composites [27]. It was noted that impact energy increases up to a certain % age of the particles and then decreased. The reason being was-This behavior is similar to the one exhibited by the hybrid composite in case of tensile test, possibly due to the agglomeration of nanofillers due to a high concentration.

Thermoplastic composites are combination of reinforcement material and thermoplastic matrix [28]. These composites have two types on the basis of processing. In the first type, prepreg is formed by pre-impregnating fibers. Then stacking of prepreg is done using heat and pressure. While, in the second type, thermoplastic materials are present either in powder, filament or films form. In film form, layers of film and reinforcement fibers are stacked in a required manner and then hot pressing is done. This technique is suitable for 2D woven thermoplastic composites. Whereas, in filament form, co-weaving, co-braiding, co-knitting or commingling is done first then hot pressing is done [29].

One drawback of molten thermoplastic polymers is their higher viscosity (500-5000 Pa·s in comparison to 100 Pa·s) than thermosets. It is very difficult to process and infuse these highly viscous materials into reinforcement materials especially in 3D composite. So, intermediate mixing of thermoplastic polymer with reinforcement fiber is done using a commingling technique to solve the problem of impregnation of fibers for 3D woven thermoplastic composites [30]. If thermoplastic matrix is used, total energy absorption of composites increases due to broad plastic deformation and debonding of matrix material from reinforcement [31].

To the best of our knowledge, no study was found on the optimization of the fabrication process and impact properties of hybrid composites made from para-aramid (PA), polyvinyl butyral (PVB) and micro fillers. In this work, PA/ PVB prepreg were developed with several percentages of silica particles and glass microspheres (1-4 %) and converted to composites using compression molding techniques. Flexural (3-point), pendulum (Charpy) and drop weight impact testing of para-aramid/PVB thermoplastic composites were performed, and results were analyzed. One-way ANOVA (Tukey) statistical analysis was used to check the significance of the results.

Experimental

Composite Fabrication

Taparan (para-arramid of Yantai Tayho Advanced materials Co. Ltd., China) supplied by iTextiles Ltd. Karachi-Pakistan was used as reinforcement. The counts of warp and weft was 1000 Denier while ends/cm and pick/cm were equal to 15/ cm each. Areal density of this ballistic grade Para aramid plain woven fabric was found equal to 340 g/m^2. The reinforcement fabric used, and its structure is shown in

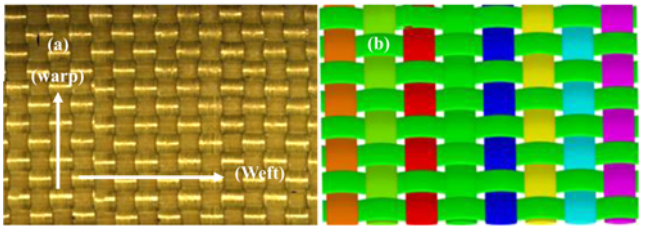

Figure 1. (a) Surface of plain-woven fabric and (b) schematic of plain weave.

			Size (d. nm)	Intensity(%)	St. Dev (d.nm)
Z-Average	3655	Peak 1	4276	100	669.8
PdI	0.254	Peak 2	0.000	0	0.000
Intercept	0.791	Peak 3	0.000	0	0.000
Result quality	Refer to quality report				

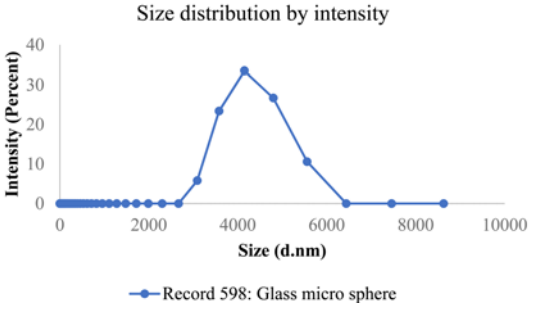

			Size (d. nm)	Intensity(%)	St. Dev (d.nm)
Z-Average	532.7	Peak 1	554.5	91.8	278.6
PdI	0.418	Peak 2	5017	8.2	601.1
Intercept	0.834	Peak 3	0.000	0	0.000
Result quality	Good				

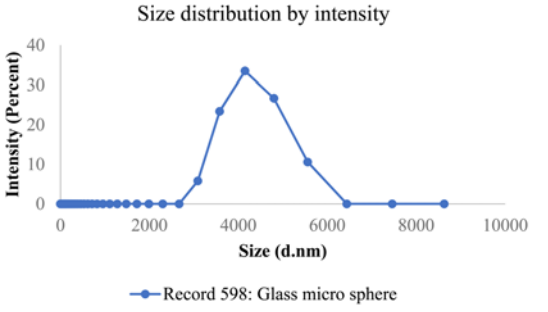

Figure 2. Particle size of (a) GMS and (b) SMP.

Figure 1.

Polyvinyl butyral (PVB), a thermoplastic matrix, supplied by Tanyun Junrong (Liaoning) Chemical Research Institute New Materials Incubator Co., Ltd. China was used for composite fabrication. It is in white powder form. In addition to para-aramid, particulate reinforcements were also used as secondary reinforcement to enhance the impact properties of the composite. Glass microspheres (GMS) supplied by Sigma Aldrich Co., Ltd. (St. Louis-United States of America) and silica micro particles (SMP) supplied by UniChem chemical reagents ltd. (Kaišiadorys-Luthuania) were used in four different percentages. These average particles sizes of GMS and SMP are shown in Figure 2. The silica particles have two peaks with 554.5 nm and 5017 nm, also most of the particles lie in the 554.5 nm region. GMS has one peak with 4276 nm size and almost all the particles lies in this region.

Also, the microscopic images of the GMS and SMP are shown in Figure 3(a) and (b) and Figure 3(c) and (d) respectively.

All the composite samples were developed using plain woven Taparan fabric having areal density (g/m^2) 340±3. In a first step the Taparan (para aramid) fabric was cut in 26 cm×26 cm size with the help of electronic cutter. The

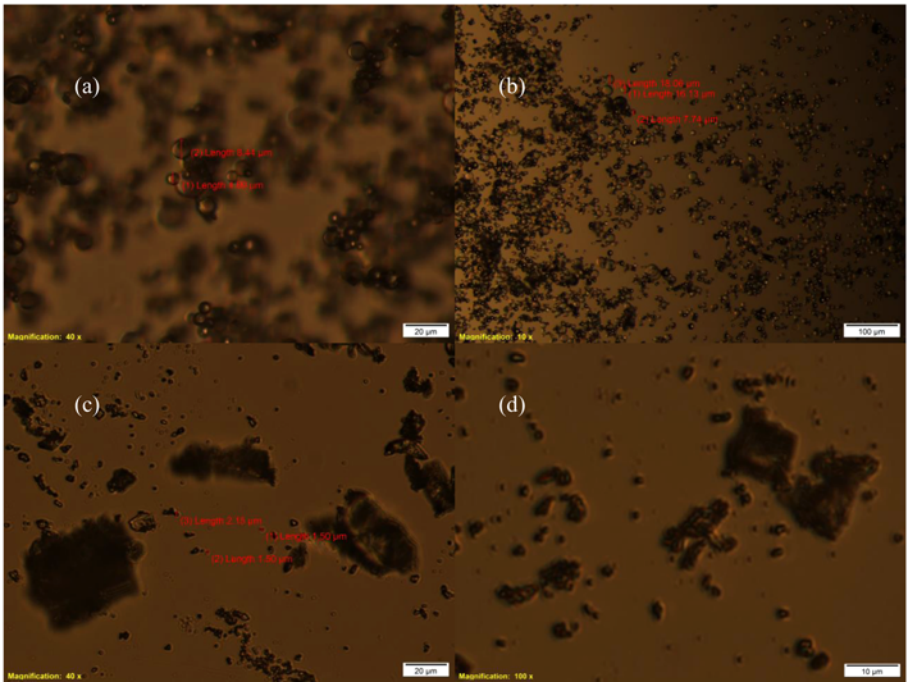

Figure 3. Microscopic images of (a, b) GMS and (c, d) SMP.

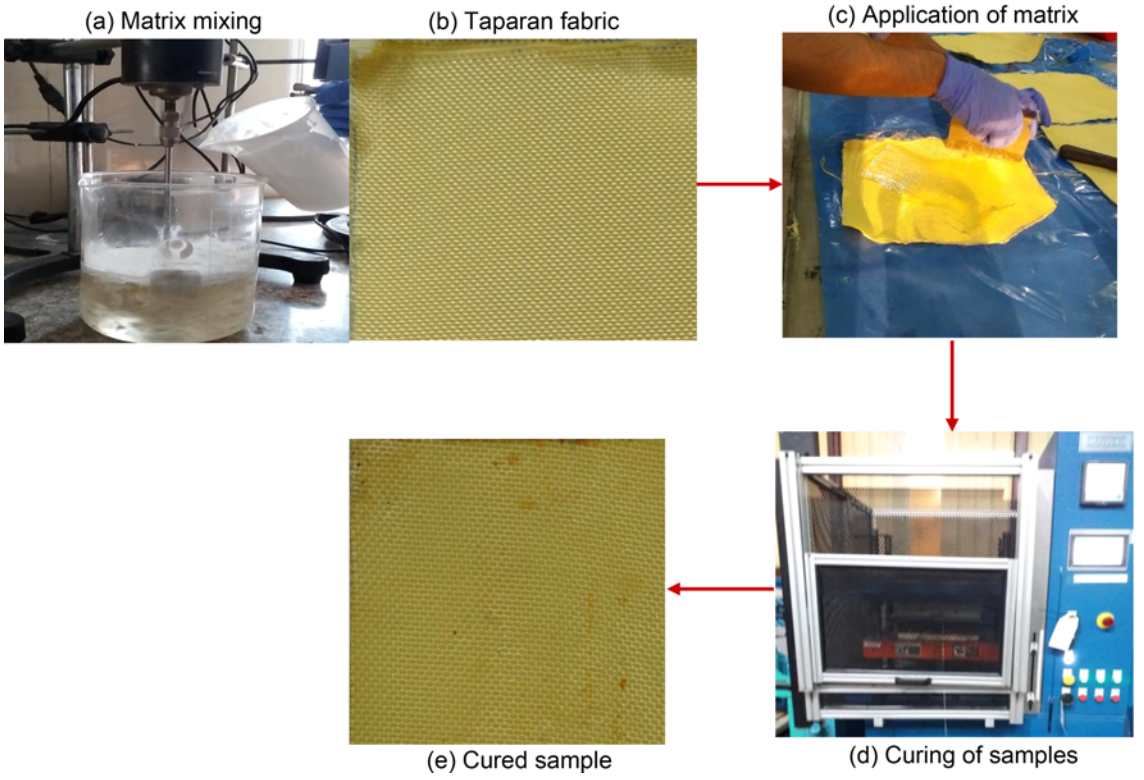

Figure 4. Composite fabrication process flow.

solution of the matrix was prepared in dimethyl formamide (DMF) by taking 700 m*l* of solvent and 300 grams of PVB. Mixing was done with the help of mechanical stirrer and PVB added slowly in the solvent. After mixing of PVB, the GMS and SMP were added in the solution separately in separate bowls. Then the fabric layers were laid down one by one and matrix solution including micro particles was applied on these layers by hand lay-up method. After hand lay-up the sample was placed inside the hot press at 180 °C and under 2 tons pressure for 25 minutes to get the cured composite. The complete composite fabrication process is shown in Figure 4. In the same way all the samples were prepared by mixing different percentages (1 %, 2 %, 3 % and 4 %) of SMP and GMS on the weight of PVB resin. One reference sample was also prepared without particles termed as 0 %. Also, fiber volume fraction for the composites was calculated using the equation (1). The design of experiments of all the samples is given in Table 1.

$$V_f = \frac{\frac{m_f}{d_f}}{\frac{m_f}{d_f}+\frac{m_r}{d_r}+\frac{m_p}{d_p}} \quad (1)$$

Table 1. Design of experiment of composites

Sample code	GMS (% age) (on the weight of resin)	SMP (% age) (on the weight of resin)
S1	1	
S2	2	
S3	3	
S4	4	
G0/S0	0	0
G1		1
G2		2
G3		3
G4		4

Testing

Three different types of mechanical testing i.e., flexural (3-point bending), pendulum (Charpy) impact and drop weight impact of the developed composite samples was done. Flexural properties of the manufactured samples was tested as per ASTM D7264 [32] with a sample size of 120 mm×13 mm on Universal Testing Machine (Z100 All-round, Zwick). The machine along with testing jaws and sample is shown in Figure 5.

Impact strength of the samples was tested on the pendulum (Charpy) impact tester (Test form) with a sample size of 80 mm×10 mm as per ISO 179 testing standard [33]. The Charpy impact test fixture and machine were shown in Figure 6.

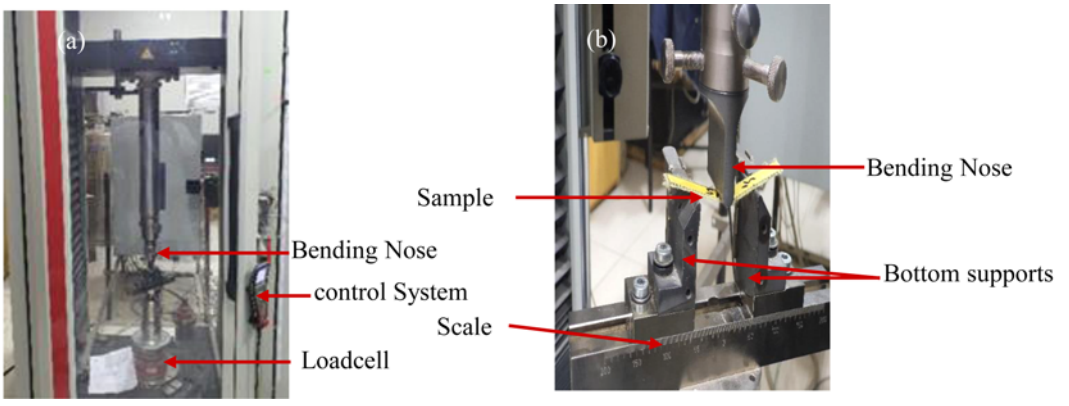

Figure 5. (a) Universal testing machine and (b) 3-point bending Jaws.

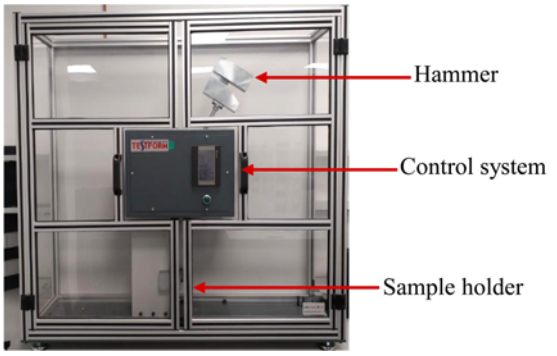

Figure 6. Charpy impact testing machine.

Furthermore developed samples were tested on a drop weight testing machine to check its impact properties as per standard ISO 6603 with a sample size of 6 inches×4 inches [34]. The drop weight fixture and machine are shown in Figure 7.

Results and Discussion

Flexural Testing (3-point)

The results of 3-point bending test showed that with the addition of silica and GMS the flexural strength of the composite increase directly with the increasing percentage of particles. This increase in flexural strength is due to formation of the local composite at the particle level. As the percentage of GMS and SMP was increased from 1 to 4 percent the local composite formation and adhesion increases, which ultimately results in an increase of flexural strength. By adding 1 percent SMP flexural strength increased 43 % as compared to zero percent SMP. Addition of 2 %, 3 % and 4 % SMP increased the flexural strength 77 %, 134 % and 143 % respectively, as compared to 0 % SMP composite sample. By adding 1 % GMS flexural strength increased 24 % as compared to 0 % GMS. Addition of 2 %, 3 % and 4 % GMS, increased the flexural strength 55 %, 74 % and 86 % respectively as compared to 0 % GMS

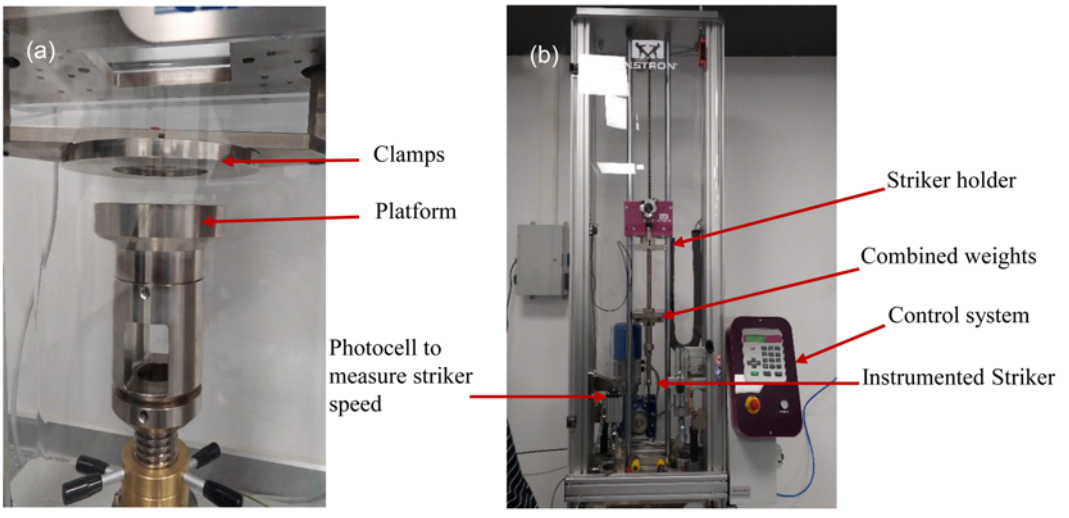

Figure 7. (a) Clamps for drop weight testing and (b) drop weight impact testing machine.

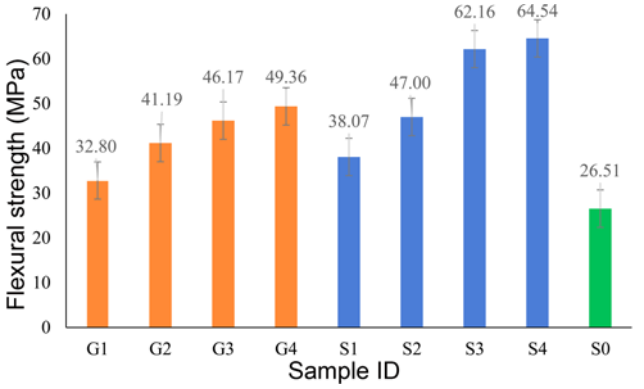

Figure 8. Flexural strength of without particles, GMS, and SMP based composites.

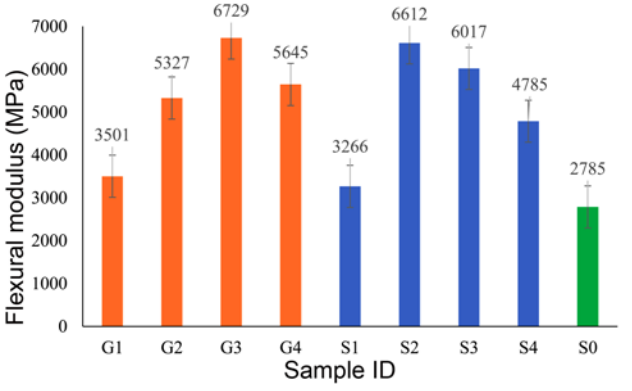

Figure 9. Flexural modulus of without particles, GMS, and SMP based composites.

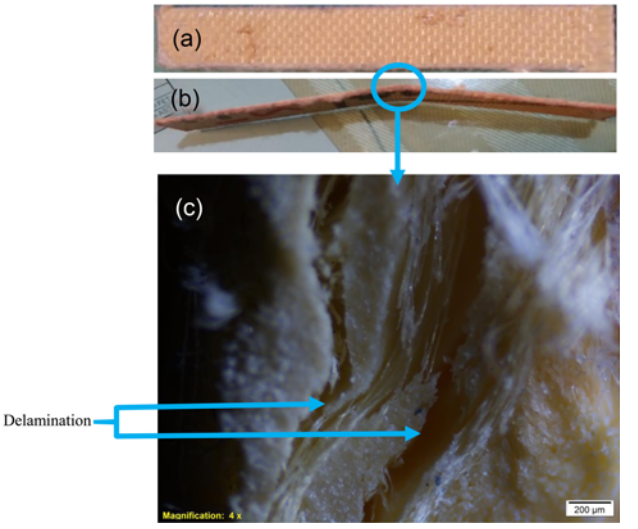

Figure 10. 3-point bending sample; (a) before testing and (b) after testing (c) Microscopic image.

composite sample. In this way 4 % of GMS and SMP showed best results. Flexural modulus increases 26 %, 91 %, 141 % and 102 % by adding 1 %, 2 %, 3 % and 4 % GMS respectively as compared to 0 % GMS and similar trend was observed in the literature [1]. By adding 1 %, 2 %, 3 % and 4 % SMP the flexural modulus increases 17 %, 137 %, 116 % and 71 % respectively as compared to 0 % SMP. While in case of flexural modulus up to 3 % of both GMS and SMP the results showed the same increasing trend in flexural modulus and with the addition of 4 %, it decreases due to over occupation of surface area, agglomeration formation and reduction in adhesion. Flexural strength and flexural modulus results of GMS and SMP are shown in Figure 8 and Figure 9, respectively.

The samples of 3-point bending before testing, after testing and microscopic view are shown in Figure 10(a), Figure 10(b) and Figure 10(c) respectively. In Figure 10(c) it is clearly seen the delamination of composite layers which results in more flexural strength.

Statistical Analysis

Analysis of variance results and model summaries (R-squares) of One-Way ANOVA (Tukey) statistical analysis of flexural strength (MPa) and modulus (MPa) are given in Table 2 and Table 3 respectively. Analysis was performed against each test result separately and outcomes were recorded. P-values showed that with the change in the GMS and SMP percentages, flexural testing results i.e., flexural strength and modulus were also changed. This change in the

Table 2. Analysis of variance results of flexural strength and modulus

		GMS percentage					SMP percentage				
	Source	DF	Adj SS	Adj MS	F-value	P-value	DF	Adj SS	Adj MS	F-value	P-value
Flexural strength (MPa)	Factor	4	1076.23	269.059	736.76	0.000	4	2999.15	749.787	1488.02	0.000
	Error	10	3.65	0.365			10	5.04	0.504		
	Total	14	1079.89				14	3004.19			
Flexural modulus (MPa)	Factor	4	31532896	7883224	3409.31	0.000	4	33502805	8375701	2219.67	0.000
	Error	10	23123	2312			10	37734	3773		
	Total	14	31556019				14	33540539			

DF: degree of freedom, SS: sum of squares, MS: mean squares.

Table 3. Model summaries of flexural strength and modulus

		S	R-square	R-square (adj)	R-square (pred)
Flexural strength (MPa)	GMS (% age)	0.604309	99.66 %	99.53 %	99.24 %
	SMP (% age)	0.709847	99.83 %	99.77 %	99.62 %
Flexural modulus (MPa)	GMS (% age)	48.0860	99.93 %	99.90 %	99.84 %
	SMP (% age)	61.4280	99.89 %	99.84 %	99.75 %

results was statistically significant because the p-value for each response was less than 0.05. Furthermore, p-value for each flexural testing result was equal to zero, which showed that effect of change in GMS and SMP on each test result was highly significant. Moreover, R-square (coefficient of determination) percentages against each result were more than 99 % for both GMS and SMP as given in Table 3. The R - square is the percentage of variation in the response that is explained by the model. So, the higher the percentage of R-square during statistical analysis, higher will be the accuracy and dependencies of the model.

Interval and Tukey simultaneous plots for flexural strength for both GMS and SMP are shown in Figure 11. Interval plot showed the range of results for flexural strength while Tukey comparison results are used to formally test whether the difference between a pair of groups is statistically significant. The interval plot for GMS and SMP in Figure 11(a) and Figure 11(c) respectively, showed that none of the five (5) intervals was overlapping with each other highlighting the difference in means of all these intervals were significantly different.

The Tukey plots for flexural strength of GMS and SMP are shown in Figure 11(b) and Figure 11(d). The Tukey plot shows that the confidence intervals for those differences between the means, which do not include zero in their range are significant. All the confidence intervals for GMS and SMP as shown in Figure 11(b) and Figure 11(d) did not include zero in the pair of means, which showed that the differences between the pair of means were significant. So, the effect of change in GMS and SMP on the flexural strength was statistically significant.

Interval and Tukey simultaneous plots for flexural modulus for both GMS and SMP are shown in Figure 12. The interval plot for GMS and SMP in Figure 12(a) and Figure 12(c) respectively, showed that none of the five (5) intervals was overlapping with each other highlighting the difference in means of all these intervals were significantly different. The Tukey plots for flexural modulus of GMS and SMP are shown in Figure 12(b) and Figure 12(d). All the confidence intervals for GMS and SMP as shown in Figure 12(b) and Figure 12(d) did not include zero in the pair of means, which showed that the differences between the pair

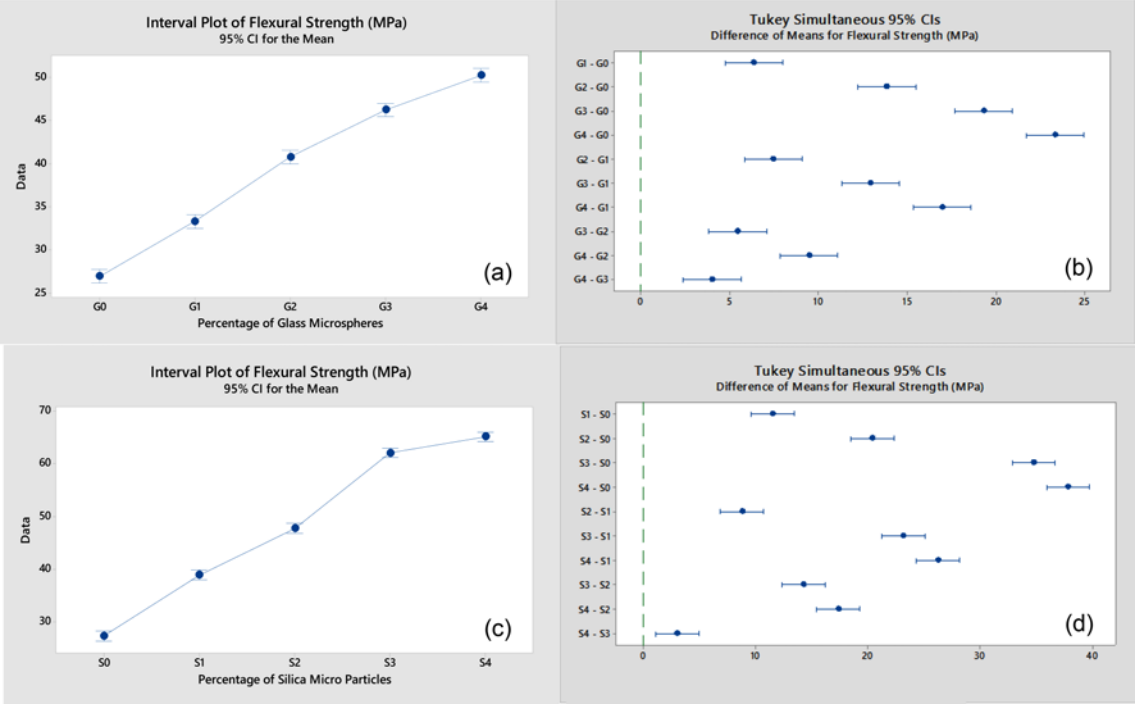

Figure 11. Flexural strength: GMS (a) interval plot, (b) Tukey simultaneous plot, and SMP, (c) interval plot, (d) Tukey simultaneous plot.

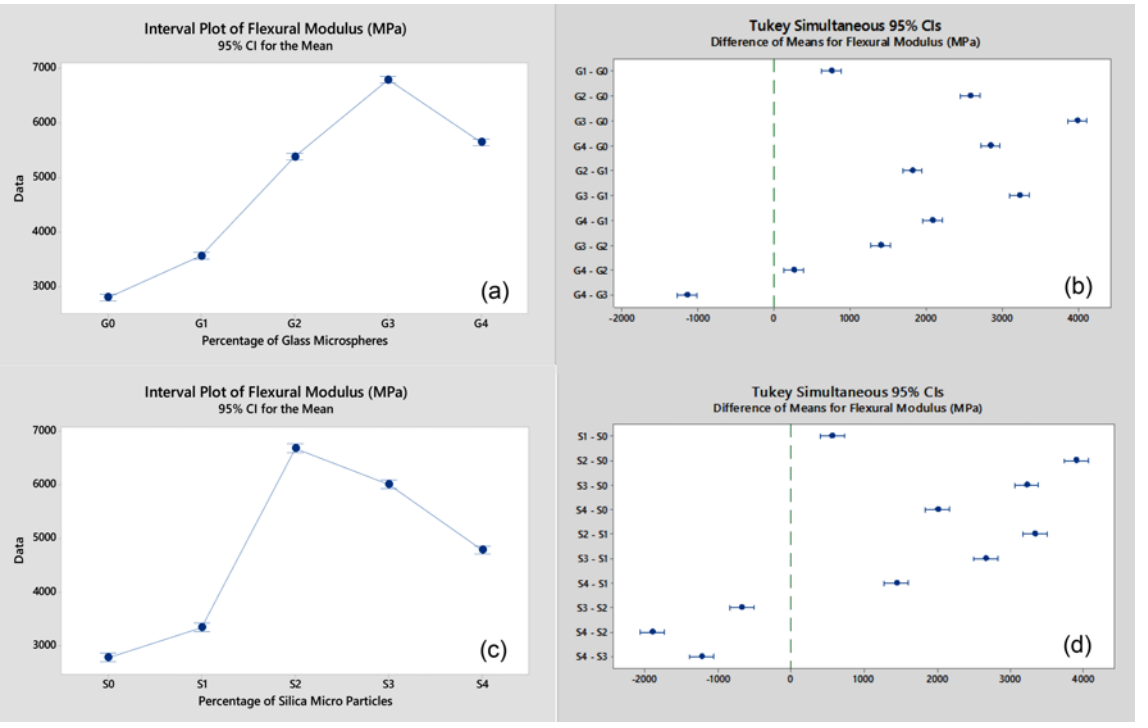

Figure 12. Flexural modulus: GMS (a) interval plot, (b) Tukey simultaneous plot, and SMP, (c) interval plot, (d) Tukey simultaneous plot.

of means were significant. So, the effect of change in GMS and SMP on the flexural modulus was statistically significant.

Pendulum (Charpy) Impact Testing

The results of Charpy impact show that with the addition of GMS the impact strength increases directly with the increase in percentage of GMS up to 3 % but at 4 % it decreases. While in case of SMP the impact energy increases up to 2 % addition of the particles. By adding 3 % impact energy decreases due to agglomeration. Again, at 4 % it increases, but still, it is less than 2 % SMP composite results. First the impact strength increases due to local composite formation with particles and more adhesion after that due to agglomeration it decreases. In case of GMS the impact energy absorbed with 1 % addition of GMS increased from 30.6 kJ/m^2 to 39.97 kJ/m^2 which is 30 % more in comparison to 0 % GMS. While by adding 2 %, 3 % and 4 % GMS there is 49 %, 76 % and 69 % increase in absorbed energy respectively in comparison to 0 % GMS. When we add 1 % SMP impact energy increased from 24.5 kJ/m^2 to 33.91 kJ/m^2 which is 38 % more than 0 % SMP composite sample. By adding further 2 %, 3 % and 4 % SMP absorbed energy increases 86 %, 61 % and 72 % respectively in comparison to 0 % SMP. So, GMS particles showed best results at 3 % and SMP showed best results at 2 % having absorbed energy

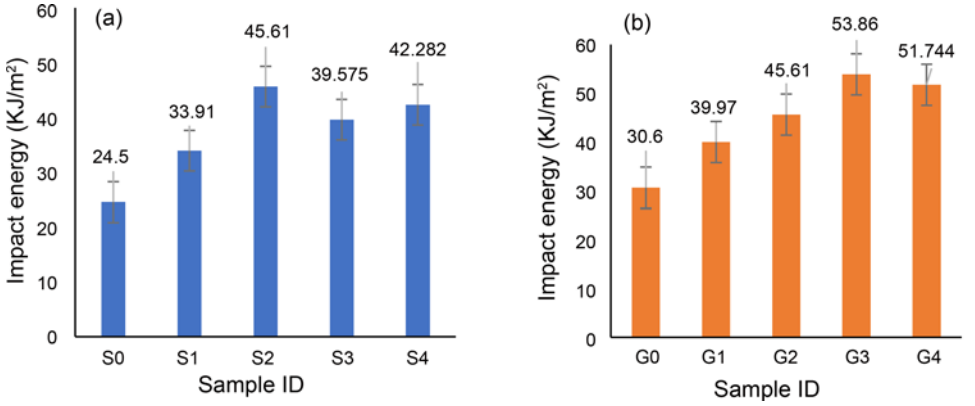

Figure 13. Energy absorbed with (a) SMP and (b) GMS PA/PVB composites.

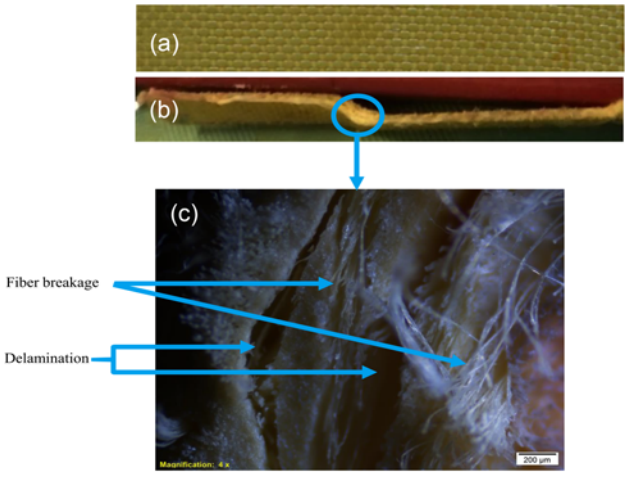

Figure 14. Charpy impact samples; (a) before testing, (b) after testing, and (c) microscopic image.

53.86 kJ/m^2 and 45.61 kJ/m^2 respectively [1]. The energy absorption results of GMS and SMP composites are shown in Figure 13(a) and Figure 13(b) respectively.

The samples for Charpy impact before testing, after testing and microscopic images after impact testing are shown in Figure 14(a), Figure 14(b), and Figure 14(c) respectively.

Statistical Analysis

Analysis of variance results and model summaries (R-squares) of One-Way ANOVA (Tukey) statistical analysis of Charpy impact energy are given in Table 4 and Table 5 respectively. P-values showed that with the change in the GMS and SMP percentages, impact energy values were also changed. This change in the results was statistically significant because the p-value was less than 0.05. Furthermore, p-value was equal to zero, which showed that effect of change in GMS and SMP on impact energy was highly significant. Moreover, R-square percentages against impact energy were more than 99 % for both GMS and SMP as given in Table 5. Higher the percentage of R-square during statistical analysis, higher will be the accuracy and dependencies of the model.

Interval and Tukey simultaneous plots of Charpy impact energy for both GMS and SMP are shown in Figure 15. The interval plot for GMS and SMP in Figure 15(a) and Figure 15(c) respectively, showed that none of the five (5) intervals was overlapping with each other highlighting the difference in means of all these intervals were significantly different. The Tukey plots for impact energy of GMS and SMP are shown in Figure 15(b) and Figure 15(d). The All the confidence intervals for GMS and SMP as shown in Figure 15(b) and Figure 15(d) did not include zero in the pair of means, which showed that the differences between the pair of means were significant. So, the effect of change in GMS and SMP on the impact energy was statistically significant.

Drop Weight Impact Testing

Composite sample without particles the maximum force value was 1200 N while displacement was 8 mm. As we added the SMP in the PA/PVB composite sample the force was increased up to 3500 N and displacement was also increased up to 10 mm. By further increasing the particle percentage, the similar increasing trend of force was observed. Also, by GMS in the composite sample, the similar increasing trend of force was found. Force verses displacement curves of SMP and GMS composites are shown in Figure 16(a) and Figure 16(b) respectively.

Similarly, the force verses time curves showed the similar behavior as in force verses displacement curves of both GMS and SMP. Force verses time of SMP and GMS composites are shown in Figure 17(a) and Figure 17(b) respectively.

The absorbed energy versus displacement curves of PA/PVB composite samples with different percentage (0 %, 1 %, 2 %, 3 % and 4 %) of SMP and GMS are shown in Figure 18(a) and Figure 18(b) respectively. 3 % SMP and GMS composites showed the highest value of absorbed energy [35,36].

Table 4. Analysis of variance results of Charpy impact energy

	Source	GMS percentage					SMP percentage				
		DF	Adj SS	Adj MS	F-value	P-value	DF	Adj SS	Adj MS	F-value	P-value
Impact energy (kJ/m^2)	Factor	4	1054.88	263.720	435.71	0.000	4	826.551	206.638	324.77	0.000
	Error	10	6.05	0.605			10	6.363	0.636		
	Total	14	1060.93				14	832.914			

DF: degree of freedom, SS: sum of squares, MS: mean squares.

Table 5. Model summaries of impact energy

		S	R-square	R-square (adj)	R-square (pred)
Impact energy (kJ/m^2)	GMS (%age)	0.777989	99.43 %	99.20 %	98.72 %
	SMP (%age)	0.797655	99.24 %	98.93 %	98.28 %

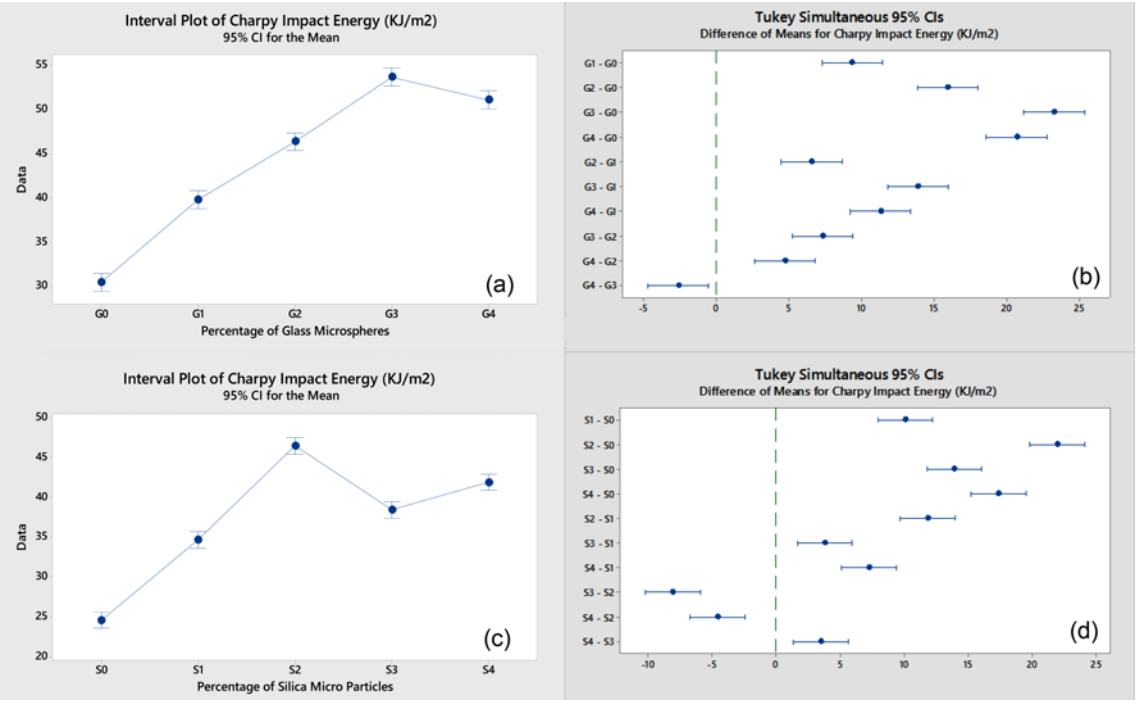

Figure 15. Impact energy (Charpy): GMS (a) interval plot, (b) Tukey simultaneous plot, and SMP, (c) interval plot, (d) Tukey simultaneous plot.

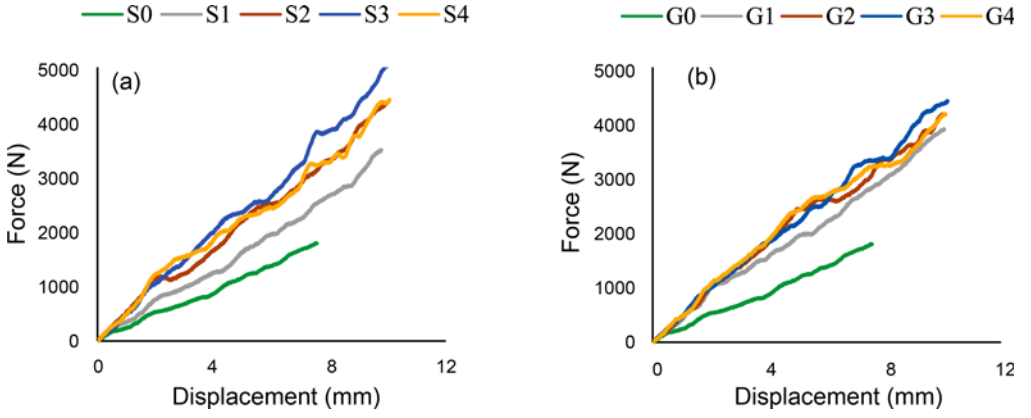

Figure 16. Force verses displacement of (a) SMP and (b) GMS composites.

Also, energy absorbed verses time curves of SMP, and GMS PA/PVB composites are shown in Figure 19(a) and Figure 19(b) respectively. It showed the similar increasing trend as in case of energy verses displacement curves.

The sample of drop weight testing before testing are shown in Figure 20(a), while after testing are shown in Figure 20(b), Figure 20(c), and Figure 20(d).

Statistical Analysis

Analysis of variance results and model summaries (R-squares) of One-Way ANOVA (Tukey) statistical analysis of maximum force and energy absorbed during drop weight impact testing are given in Table 6 and Table 7 respectively. P-values showed that with the change in the glass microspheres GMS and SMP percentages, drop weight impact testing results i.e. maximum force and energy absorbed were also changed. This change in the results was statistically significant because the p-value for each response was less than 0.05. Furthermore, p-value for each drop weight impact testing result was equal to zero, which showed that effect of change in GMS and SMP on each test result was highly significant. Moreover, R-square percentages against each result were more than 99 % for both GMS and SMP as given in Table 7.

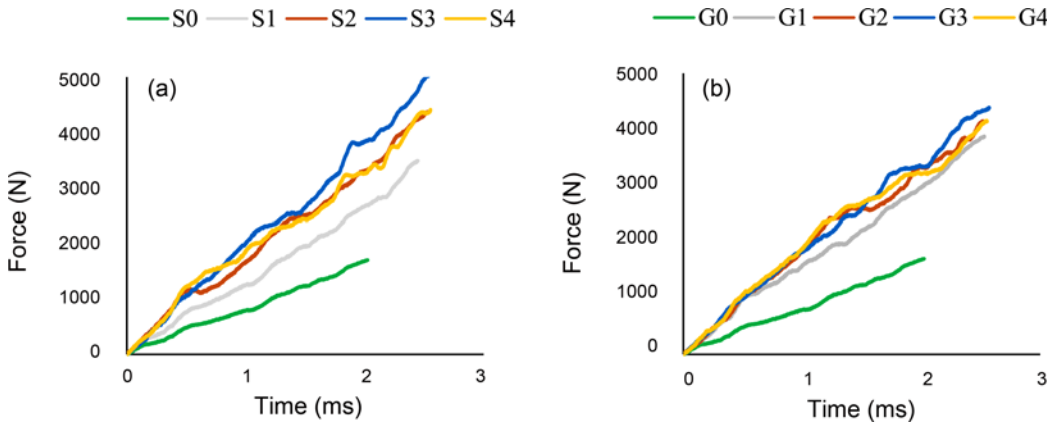

Figure 17. Force verses time curves of (a) SMP and (b) GMS PA/PVB composites.

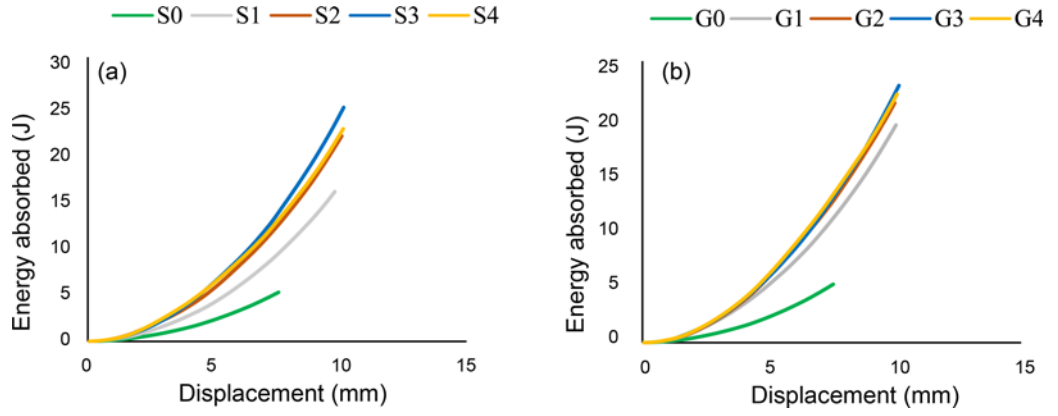

Figure 18. Energy absorbed verses displacement of (a) SMP and (b) GMS composites

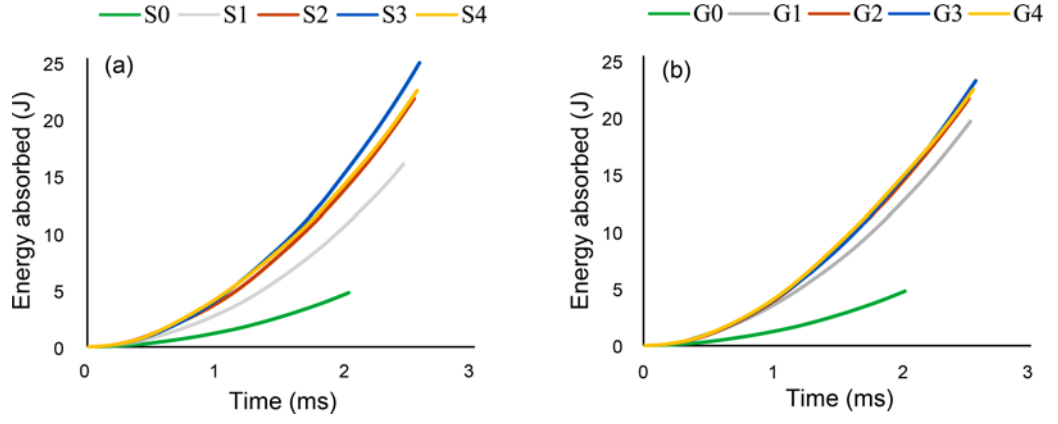

Figure 19. Energy absorbed verses time of (a) SMP and (b) GMS PA/PVB composites.

remaining confidence intervals did not include zero in the pair of means, which showed that the differences between the pair of means were significant.

Interval and Tukey simultaneous plots of absorbed energy for both GMS and SMP are shown in Figure 22. The interval plot showed that out of five (5) intervals; 3rd (G2) and 4th (G3), 3rd (G2) and 5th (G4) intervals in GMS and 3rd (S2), 5th (S4) intervals in SMP overlap each other showing the differences between the means were not statistically significant. While remaining intervals in GMS and SMP did not overlap with anyone, therefore, the difference in their means was significantly different as shown in Figure 22(a)

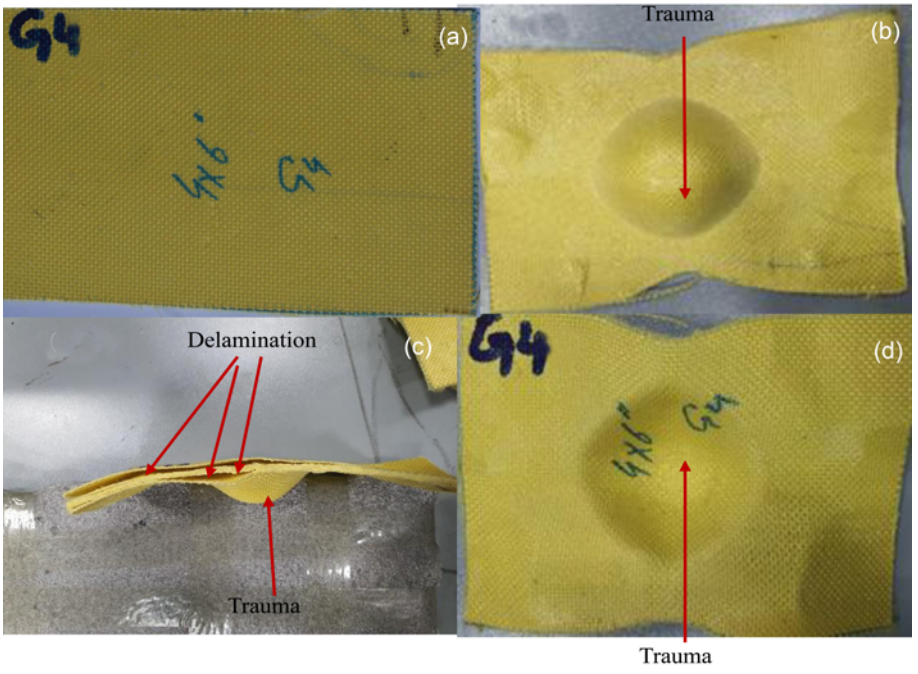

Figure 20. Drop weight samples (a) before testing and (b, c, and d) after testing.

Table 6. Analysis of variance results of maximum force and energy absorbed

		GMS percentage					SMP percentage				
	Source	DF	Adj SS	Adj MS	F-value	P-value	DF	Adj SS	Adj MS	F-value	P-value
Maximum force (N)	Factor	4	14538756	3634689	1233.49	0.000	4	18637494	4659374	2297.14	0.000
	Error	10	29467	2947			10	20283	2028		
	Total	14	14568223				14	18657777			
Energy absorbed (J)	Factor	4	689.498	172.375	2102.13	0.000	4	792.404	198.101	1217.83	0.000
	Error	10	0.820	0.082			10	1.627	0.163		
	Total	14	690.318				14	794.030			

DF: degree of freedom, SS: sum of squares, MS: mean squares.

Table 7. Model summaries of maximum force and energy absorbed

		S	R-square	R-square (adj)	R-square (pred)
Maximum force (N)	GMS (%age)	54.2832	99.80 %	99.72 %	99.54 %
	SMP (%age)	45.0370	99.89 %	99.85 %	99.76 %
Energy absorbed (J)	GMS (%age)	0.286356	99.88 %	99.83 %	99.73 %
	SMP (%age)	0.403320	99.80 %	99.71 %	99.54 %

Interval and Tukey simultaneous plots of maximum force for both GMS and SMP are shown in Figure 21. The interval plot showed that out of five (5) intervals; only 3rd (G2), 5th (G4) intervals in GMS and 3rd (S2), 5th (S4) intervals in SMP overlap each other showing the differences between the means were not statistically significant. While all remaining intervals in GMS and SMP did not overlap with anyone, therefore, the difference in their means was significantly different as shown in Figure 21(a) and Figure 21(c). Similarly, Tukey plot showed that the one (01) pair in GMS and one (01) pair in SMP include zero in the mean values of their confidence intervals as shown in Figure 21(b) and Figure 21(d), which showed that the differences between the means of these pairs were not significant. All

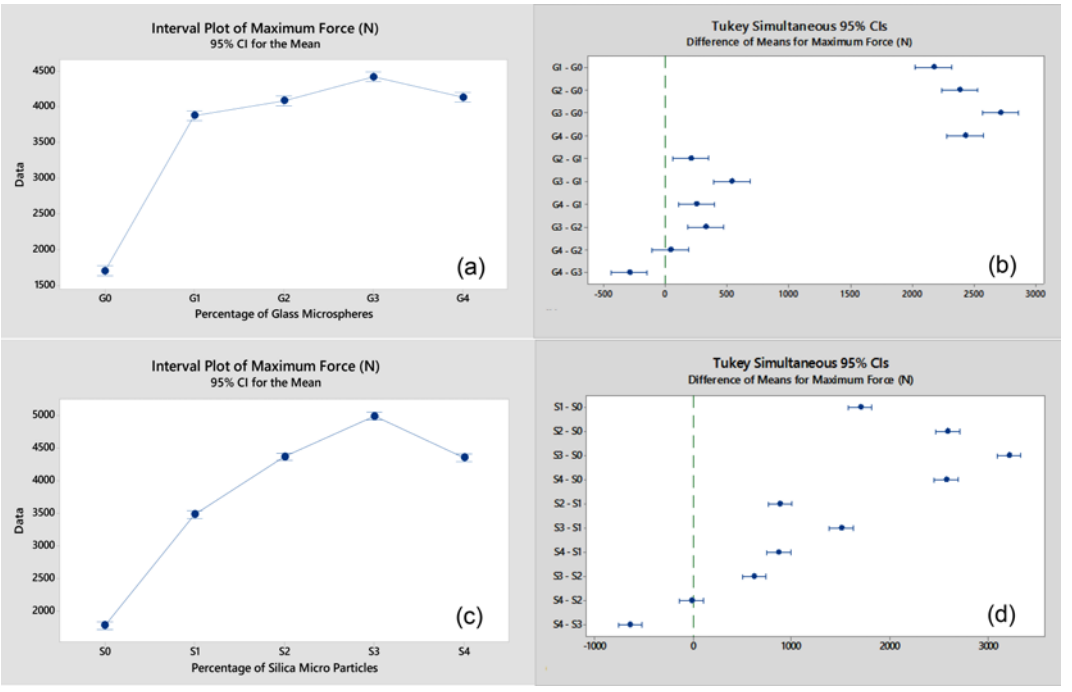

Figure 21. Maximum force (drop weight): GMS (a) interval plot, (b) Tukey simultaneous plot, and SMP, (c) interval plot, (d) Tukey simultaneous plot.

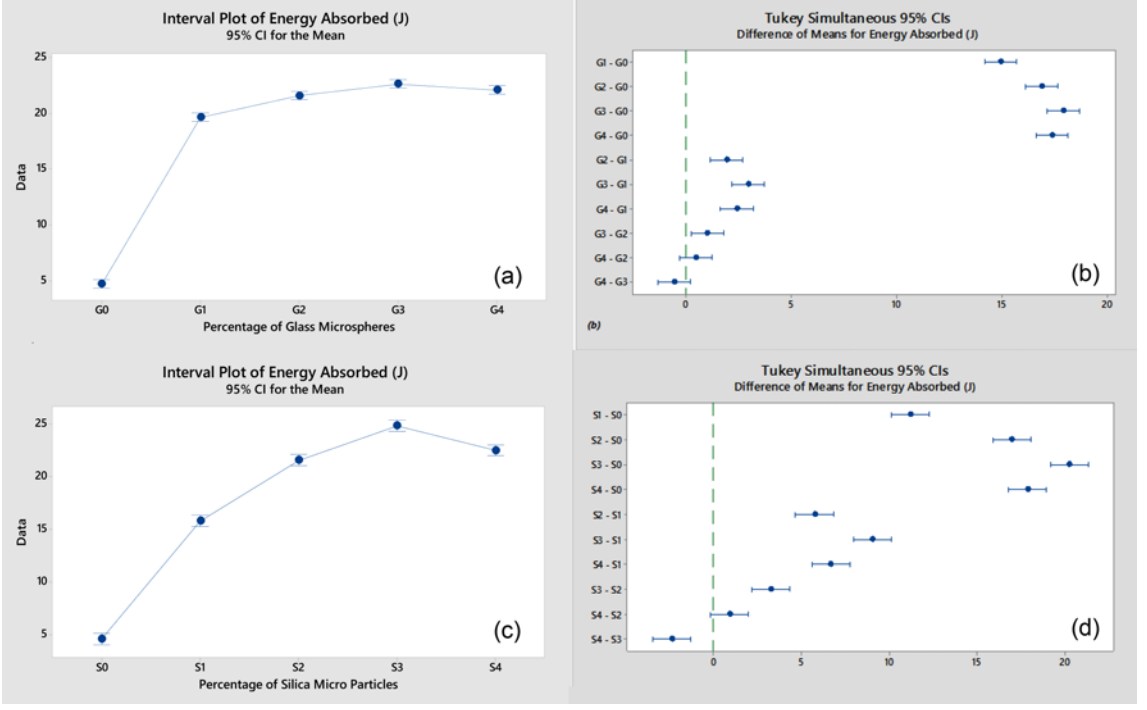

Figure 22. Energy absorbed (drop weight): GMS (a) interval plot, (b) Tukey simultaneous plot, and SMP, (c) interval plot, (d) Tukey simultaneous plot.

and Figure 22(c). Similarly, Tukey plot showed that the two (02) pairs in GMS and one (01) pair in SMP include zero in the mean values of their confidence intervals as shown in Figure 22(b) and Figure 22(d), which showed that the differences between the means of these pairs were not significant. All remaining confidence intervals did not include zero in the pair of means, which showed that the differences between the pair of means were significant.

Conclusion

1. Development of pre-preg using slurry of PVB and micro-fillers followed by the fabrication of composites on compression moulding machine found to a successful route for development of good quality thermoplastic composites for impact applications.
2. It is further concluded that flexural strength of developed composites increases with the increasing percentage of SMP and GMS up to 4 %. Flexural modulus also increases by increasing percentage of SMP and GMS up to 3 % and decreases at 4 % addition of SMP and GMS.
3. In Charpy impact the impact strength increases with the addition of Silica up to 2 % and GMS up to 3 %. With the addition of silica and GMS the impact force increases directly with increasing percentage of particles. Also, GMS based composite better energy absorption as compared to the SMP composites.
4. During drop weight impact testing maximum force and energy absorbed values were increased were the increase in the percentage of the GMS and SMP in the composites. While 3 % GMS and SMP gave the best results.
5. One-way ANOVA (Tukey) statistical analysis results showed that the change in the percentage of GMS and SMP had statistically significant effect on flexural, Charpy impact and drop weight impact testing results because the p-value was less than 0.05 for each test result. Also, R-square (coefficient of determination) percentages against each result were more than 99 % for both GMS and SMP which shows higher accuracy and dependency of the models.

Acknowledgments

Authors are thankful to the Higher Education Commission of Pakistan for Funding this research work under National Research Program for Universities (NRPU-12477).

References

1. Z. Abbas, S. Shahid, Y. Nawab, K. Shaker, and M. Umair, *Polym. Compos.*, **41**, 4771 (2020).
2. S. N. Monteiro T. L. Milanezia, L. H. L. Louroa, E. P. Lima, F. O. Bragaa, A. V. Gomes, and J. W. Drelich, *Mater. Des.*, **96**, 263 (2016).
3. J. G. Carrillo, R. G. Castellanos, and E. A. Flores-johnson, *Polym. Test.*, **31**, 512 (2012).
4. S. Naik, R. D. Dandagwhal, and P. K. Loharkar, *Mater. Today Proc.*, **21**, 1366 (2020).
5. J. G. Carrillo, R. A. Gamboa, E. A. Flores-Johnson, and P. I. Gonzalez-Chi, *Polym. Test.*, **31**, 512 (2012).
6. W. Y. W. Hanif, M. S. Risby, and M. M. Noor, *Procedia Eng.*, **114**, 118 (2015).
7. T. Guleria, N. Verma, S. Zafar, and V. Jain, *J. Reinf. Plast. Compos.*, doi: 10.1177/0731684420959449 (2020).
8. Z. Naghizadeh, M. Faezipour, M. H. Pol, G. H. Liaghat, and A. Abdolkhani, *Proc. Inst. Mech. Eng. Part L J. Mater. Des. Appl.*, **232**, 785 (2018).
9. K. Greenwood and C. R. Cork, *UMIST*, p.32, 1987.
10. P. M. Cuniff, *Text. Res. J.*, **62**, 495 (1992).
11. S. Rajesh, B. V. Ramnath, M. Abhijith, R. D. Riju, and K. K. Kishan, *Materials Today: Proceedings*, **5**, 1156 (2018).
12. A. Bhatnagar, "Lightweight Ballistic Composites", Woodhead Publishing, 2006.
13. A. K. Bandaru, S. Patel, Y. Sachan, S. Ahmad, R. Alagirusamy, and N. Bhatnagar, *Compos. Part A Appl. Sci. Manuf.*, **90**, 642 (2016).
14. A. L. Peters, M.S. Thesis, Faculty of California Polytechnic State University, CA, 2014.
15. K. Joseph, S. K. Malhotra, K. Goda, and M. S. Sreekala, *Polym. Compos.*, **21**, 16 (2012).
16. C. Dufour, P. Wang, F. Boussu, and D. Soulat, *Appl. Compos. Mater.*, **21**, 725 (2014).
17. H. R. Clauser, *Sci. Am.*, **229**, 36 (2010).
18. R. Phillips, D. A. Akyüz, and J.-A. E. Månson, *Compos. Part A Appl. Sci. Manuf.*, **29**, 395 (1998).
19. S. G. Kulkarnia, X.-L. Gaob, S. E. Hornerc, J. Q. Zhengc, and N. V. Davidd, *Compos. Struct.*, **101**, 313 (2013).
20. K. Brown, R. Brooks, and N. Warrior, "Numerical Simulation of Damage in Thermoplastic Composites Materials", Fifth European LS-DYNA Users Conference, Birmingham, 2005.
21. O. A. Khondker T. Fukui, M. Inoda, A. Nakai, and H. Hamada, *Compos. Part A Appl. Sci. Manuf.*, **35**, 1135 (2004).
22. E. Richter, K. Uhlig, A. Spickenheuer, L. Bittrich, and G. Heinrich, ECCM16-16th European Conference on Composite Materials, 2014.
23. Z. F. Zhang and X. Hu, *Mech. Compos. Mater.*, **51**, 377 (2015).
24. D. Toorchi, H. Khosravi, and E. Tohidlou, *J. Ind. Text.*, doi: 10.1177/1528083719879922 (2019).
25. E. E. Haro, A. G. Odeshi, and J. A. Szpunar, *Int. J. Impact Eng.*, **96**, 11 (2016).
26. R. Potluri, *J. Nat. Fibers*, **16**, 137 (2019).
27. M. Jabbar, M. Karahan, Y. Nawab, M. Ashraf, and T. Hussain, *J. Text. Inst.*, **110**, 606 (2019).
28. R. M. Stack and F. Lai, *Thermoforming Quarterly*, **32**, 48 (2013).

29. W. Kuo and J. Fang, *Compos. Sci. Tech.*, **60**, 643 (2000).
30. J. E. Rocher, S. Allaoui, G. Hivet, and E. Blond, 13th Autex World Textile Conference, 2013.
31. E. Selver, "Tow Level Hybridization for Damage Tolerant Composites", The University of Manchester, 2014.
32. ASTM D7264/7264M, "Standard Test Method for Flexural Properties of Polymer Matrix Composite Materials", 2015.
33. EN ISO 179, "Plastics-Determination of Charpy Impact Properties", 2000.
34. ISO 6603-1 (E), "Plastics-Determination of Puncture Impact Behaviour Rigid Plastics", 2000.
35. M. Umair, M. Hussain, Z. Abbas, K. Shaker, and Y. Nawab, *J. Compos. Mater.*, doi: 10.1177/0021998320987605 (2020).
36. A. J. Varghese and B. A. Ronald, *Silicon,* doi: 10.1007/s12633-020-00566-3 (2020).
37. Z. Naghizadeh, M. Faezipour, M. Hossein, G. H. Liaghat, and A. Abdolkhani, *Proc. IMechE Part L: J. Mater.: Des. Appl.,* **232**, 785 (2018).